Novel Dihydrofolate Reductase Inhibitors. Structure-Based versus Diversity-Based Library Design and High-Throughput Synthesis and Screening

Pierre C. Wyss,*,† Paul Gerber, Peter G. Hartman, Christian Hubschwerlen,† Hans Locher,† Hans-Peter Marty, and Martin Stahl

Preclinical Research, F. Hoffmann-La Roche Ltd., CH-4070 Basle, Switzerland

Received November 1, 2002

Novel 2,4-diaminopyrimidines bearing N,N-disubstituted aminomethyl residues at the 5-position were designed as dihydrofolate reductase (DHFR) inhibitors. These compounds were obtained by treatment of 1-[(2,4-diamino-5-pyrimidinyl)methyl]pyridinium bromide with secondary amines in a polar solvent and in the presence of triethylamine at room temperature. The procedure was found to be very efficient and suitable for application in high-throughput synthesis. In addition, we found that high-throughput screening for enzymatic and in vitro antibacterial activity could be performed on crude reaction mixtures, thus avoiding any purification step. Over 1200 proprietary secondary amines were selected for high-throughput synthesis, based on structural and diversity-related criteria, and the resulting products were submitted to high-throughput screening. A greater number of hits, and significantly more active compounds, were obtained through structure-based library design than through diversity-based library design. Different classes of inhibitors of DHFR were identified in this way, including compounds derived from di-, tri-, and tetracyclic amines. In general, these products showed high activity against the enzymes derived from both TMP-sensitive and TMP-resistant *Streptococcus pneumoniae*. Some compounds possessed appreciable selectivity for the bacterial over the human enzyme, whereas other compounds were not at all selective. In most cases, active enzyme inhibitors also displayed antibacterial activity.

Introduction

The spread of antibiotic resistance has reached alarming proportions in some species, and one of the most worrying trends is the increasing incidence of multiresistant *Staphylococcus aureus* (MRSA) in hospitals and multiresistant *Streptococcus pneumoniae* in the community.[1,2] There is therefore an urgent need for effective antibacterial agents to treat infections caused by these organisms.

The enzyme dihydrofolate reductase (DHFR) has been established clinically as a proven target for chemotherapy. The DHFR inhibitor trimethoprim (TMP, Figure 1), often used in combination with sulfamethoxazole (SMZ), was introduced primarily for the treatment of community-acquired infections and urinary tract infections, with emphasis on Gram-negative pathogens. Despite some recent work on *Pneumocystis carinii*,[3] the enzyme remains an underexploited target in the antibacterial field, and no optimization of inhibitors against Gram-positive pathogens has been performed.

As part of a previous program, we designed and synthesized a large number of 5-benzyl-2,4-pyrimidinediamines incorporating lipophilic substituents in the 3′-position of the benzene nucleus with the objective of seeking derivatives with antibacterial activity against highly resistant Gram-positive organisms, particularly against *S. aureus*. The best compounds identified, e.g., RO-64-5781, showed inhibitory activity that was up to 190 000 times greater than that of TMP, allowing the coverage of TMP-resistant strains, and selectivity was at least as good as that of TMP.[4] These new compounds were highly active in vitro against all staphylococci, including TMP-resistant strains, and showed good antistaphylococcal activity in a mouse septicaemia model after parenteral application. However, the high level of binding to plasma proteins exhibited by these compounds, coupled with a low solubility, has caused problems in achieving their formulation at the dose estimated to be required for clinical use. The high lipophilicity and molecular weight of these compounds may be responsible for their unfavorable physicochemical properties. In an attempt to solve these problems, we decided to design inhibitors of different structural classes and reduced molecular size.

Information available from crystal structures of DHFR and complexes with inhibitors has shown that the 2,4-diaminopyrimidine moiety of TMP fits nearly ideally into a narrow pocket in the active site of the enzyme.[5,6] As all previous efforts aimed at replacing this moiety have so far failed, we decided to retain the 2,4-diaminopyrimidine "needle" fragment[7] and to focus our efforts to structure modifications of the side chain at the 5-position of the 2,4-diaminopyrimidine moiety.

Rationale

We hypothesized that 2,4-diaminopyrimidine derivatives incorporating basic N-disubstituted aminomethyl residues at the 5-position (**1**) might have better solubility properties than TMP itself. Moreover, we anticipated that an appropriate selection of candidates from the

* To whom correspondence should be addressed. Address: Morphochem AG, Schwarzwaldallee 215, CH-4058 Basle, Switzerland. Phone: ++41-61-695 21 39. Fax: ++41-61-695 21 22. E-mail: pierre.wyss@morphochem.ch.

† Present address: Morphochem AG, Schwarzwaldallee 215, CH-4058 Basle, Switzerland.

10.1021/jm020495y CCC: $25.00
Published on Web 05/08/2003

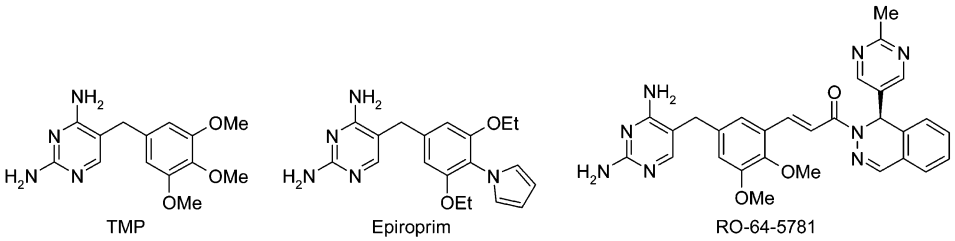

Figure 1. Inhibitors of DHFR containing 2,4-diaminopyrimidine moieties.

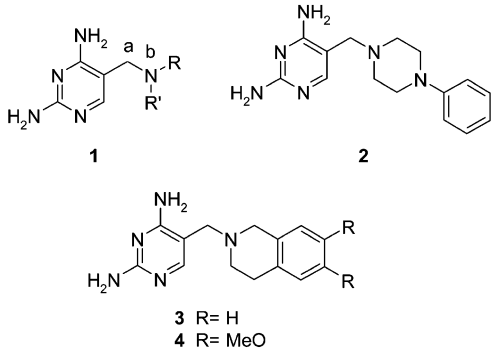

Figure 2. General structure of designed inhibitors (**1**) and examples of analogues known before initiating this work (**2**−**4**).

large pool of available amines would allow modulation of the pK_a and clogP properties of the resulting products and thereby influence penetration into bacteria and the antibacterial properties of the compounds.

Only a limited number of pyrimidines of type **1** (Figure 2) have been described so far in the literature. For instance, Godel et al. have synthesized compounds derived from substituted and unsubstituted piperazines (e.g., **2**) and piperidines as antagonists of the dopamine D4 receptor.[8] The unsubstituted 1,2,3,4-tetrahydroisoquinoline **3** is mentioned in a patent of the Wellcome Foundation on antibacterial pyrimidine compounds.[9] However, this compound was found to be inactive in our DHFR and in vitro antibacterial assays. In the first step, we prepared a limited number of compounds of type **1** and, interestingly, one of the first compounds synthesized in this series (**4**) showed an appreciable inhibitory activity against TMP-resistant DHFR from *Streptococcus pneumoniae* but less activity against *S. aureus* (Table 1).

Table 1. Inhibition of TMP-Resistant DHFR from *S. aureus* and *S. pneumoniae* and Antibacterial Activity of Compound **4** Compared to Those of TMP

	IC_{50} (μM)		MIC (μg/mL)		
compd	S1[a]	Sp1[b]	Sa 157[c]	Spn[d]	Sp 1/1[e]
TMP	19	34	>32	2	>64
4	>100	0.21	>32	0.5	4

[a] S1, TMP-resistant DHFR from *Staphylococcus aureus* 157/4696. [b] Sp1, TMP-resistant DHFR from *Streptococcus pneumoniae* 1/1. [c] Sa 157, *Staphylococcus aureus* 157/4696 (TMP-resistant). [d] Spn, *Streptococcus pneumoniae* ATCC 49619 (TMP-susceptible). [e] Sp 1/1, *Streptococcus pneumoniae* 1/1 (TMP-resistant).

Results and Discussion

Chemistry. The first representatives of this new class of N-substituted 5-(aminomethyl)-2,4-pyrimidinediamines were initially obtained by treating 5-(bromomethyl)-2,4-pyrimidinediamine dihydrobromide (**5**) with a number of primary, secondary, and cyclic amines, as shown in Scheme 1. The starting material **5** was prepared in four steps following essentially the procedures described in the literature.[10−13] We soon realized that the insolubility of compound **5** in most usual solvents, including DMF and DMSO, and its high reactivity, often leading to complex mixtures of products, would probably limit the potential of the method. In contrast, the crystalline pyridinium salt **6**, obtained on treatment of compound **5** with pyridine in DMF, was found to be a very effective starting material for performing the nucleophilic substitutions described above. In contrast to most quaternary salts, this compound was found to be nonhygroscopic. Moreover, it is stable, very soluble in polar solvents, including DMF, DMSO, and methanol, and reactions with amines are much cleaner than the corresponding reactions previously performed using bromide **5** as a starting material.

High-Throughput Synthesis and Screening. On the basis of the interesting biological results obtained for **4**, we decided to synthesize a large number of diverse compounds of type **1** in order to identify a large variety of chemical classes exhibiting biological activity in the first hit. For this purpose, over 9000 secondary amines were extracted from the Roche proprietary library. The

Scheme 1. General Strategy for the Synthesis of 2,4-Diaminopyrimidines[a]

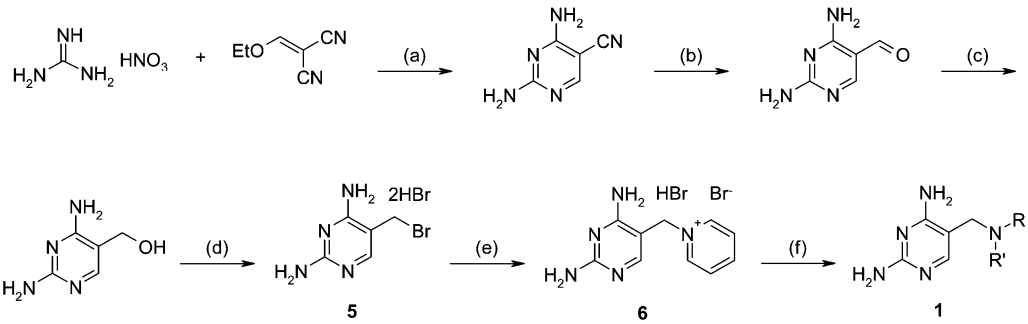

[a] Conditions: (a) NaOEt, EtOH, 20 °C, 18 h (100%); (b) Ni−Al (1:1), HCO_2H, 110 °C, 2 h (59%); (c) $NaBH_4$, H_2O, 50 °C, 4 h (86%); (d) HBr, AcOH, 95 °C, 2 h (93%); (e) pyridine, DMF, 20 °C, 2 h (96%); (f) RR′NH (1 equiv), Et_3N (5 equiv), DMF, 20 °C, 18 h.

Table 2. Inhibitors of DHFR Identified in Libraries

library no.	selection procedure	size	inhibitors *n* (%)
1	structure-based, top-score	252	54 (21)
2	structure-based, low-score or no docking solution	269	4 (1)
3	diversity-based	501	17 (3)
4	analogues of hits[a]	370	90 (24)

[a] Hits identified in library no. 1.

first selection of approximately 500 candidates was made according to the two selection criteria discussed below in the library design section. A number of preliminary experiments, including TLC and HPLC controls, showed that it is possible to perform the reaction efficiently on a 0.35−0.7 μM scale. It was initially planned to purify the crude reaction mixtures by HPLC before submitting the compounds for measuring the inhibition of DHFR enzymes and in vitro activity against Gram-positive bacteria. Fortunately enough, we found that this time-consuming operation was not required. A number of control experiments showed that neither starting materials (amines and pyridinium salt **6**), released pyridine, triethylamine, nor solvent (MeOH) interfered in any way with the biological assays under the chosen test conditions. Eighty different reactions were run in parallel on a single standard 96-well plate. Each plate included samples of TMP and epiroprim as biological references, and one reference reaction known to give an active compound was performed as well, as an internal control of the reaction. A total of 1392 compounds, included in libraries nos. 1−4 (Table 2), were prepared according to this method and evaluated for DHFR inhibition and antibacterial activity.

All compounds obtained by high-throughput synthesis were evaluated for inhibition of human DHFR and the bacterial enzymes from TMP-sensitive *S. aureus* (ATCC 25923) and TMP-resistant *S. pneumoniae* (1/1), which are denoted human, Sa, and Sp1, respectively, in the tables. Active compounds were also tested against TMP-resistant S1 DHFR from *S. aureus* and TMP-sensitive Spn DHFR from *S. pneumoniae*. Screening for antibacterial activity was performed using the following four bacterial strains: TMP-susceptible (ATCC 25923) and TMP-highly resistant *S. aureus* (157/4696), TMP-susceptible (ATCC 49619) and TMP-resistant *S. pneumoniae* (1/1). In addition, TMP-susceptible *S. aureus* was tested in a medium containing 10 μg/mL thymidine to test for activity that is not caused by antifolates. It is well-known that the growth inhibiting effect of antifolates is reversed in rich medium containing thymidine, since some bacteria are not dependent on de novo synthesis of thymidine but can take it up from the medium.[14] Finally, some subsets of highly hydrophobic compounds were tested in the presence of 10% human serum in order to discard highly lipophilic compounds that may act nonspecifically by damaging bacterial membranes.

Library Design. We tried to guide the synthesis by covering representative compounds of the whole library as well as specifically selecting subsets where binding affinity to DHFR could be expected to be high. Therefore, two alternative methods were applied to select compounds out of the virtual library of over 9000 theoretical compounds. One selection strategy was based on docking calculations, and the other one was based on diversity analysis.

(a) Structure-Based Compound Selection. The DHFR enzymes from different species (human, *S. aureus*, and *S. pneumoniae*) are highly homologous. The main difference at the center of the active site is the exchange of the three hydrophobic amino acids that are in contact with the 2,4-diaminopyrimidine ring of TMP on the side facing away from the cofactor NADPH. A crystal structure of *S. pneumoniae* DHFR is not available, but homology modeling indicates that the active site shape and polarity close to the 2,4-diaminopyrimidine binding site is closely related to that of *S. aureus* DHFR. The sequence alignment of human and *S. aureus* DHFR, as defined by the overlay of the available crystal structures, is shown in Figure 3. The sequence of *S. pneumoniae* DHFR has been manually aligned to these two sequences, and this alignment was used to build a homology model. Side chains of the framed sets of residues are close to the 2,4-diaminopyrimidine moiety.

Several structures of complexes between *S. aureus* DHFR and various Roche inhibitors have been resolved at Roche. No significant induced fit effects can be observed in these structures such that the receptor can be assumed to be rigid to a good approximation. Because of the rigidity of the receptor and the high similarity between the *S. aureus* and *S. pneumoniae* enzymes, we assumed that the use of a single-crystal structure of *S. aureus* DHFR should be sufficient for structure-based selection of compounds against both targets. We also reasoned that the difference between resistant and sensitive enzymes should not be relevant for docking studies, since TMP-resistance is not coupled with a change of binding mode of TMP in the enzymes and the shape of the binding site remains unchanged. For instance, the main determinant of TMP-resistance in *S. aureus* DHFR is a single mutation in the active site that leads to the loss of a hydrogen bond between ligand and receptor.[15] While this mutation does lead to weaker binding of the 2,4-diaminopyrimidine moiety, it does not alter its binding mode.

A list of 9448 secondary amines available in the Roche collection were retrieved as virtual reagents. 2,4-Diaminopyrimidine products **1** were generated with an in-house library enumeration program. Single 3D conformations of this library were generated with the program Corina[16,17] in mol2-format.[18] The protonation states of all compounds were adjusted with a rule-based in-house program. The nitrogen atom of the aminomethyl ring substituent common to all inhibitors (N_b in compound **1**, Figure 2) was not protonated, since this atom must be situated in a lipophilic environment within the DHFR binding site. For docking, the crystal structure of DHFR from TMP-sensitive *S. aureus* complexed with the Roche inhibitor RO-62-6091 (Figure 4) was chosen. The library members were docked with the constraint of a fixed position of the 2,4-diaminopyrimidine fragment taken from the crystal structure (schematic view in Figure 4). The docking program FlexX,[19−22] version 1.7.0, was used for the calculations. Default parameter settings of FlexX were used except for a modified scoring function that penalizes hydrogen bonds formed at solvent-accessible parts of the protein surface.[23] The calculation was

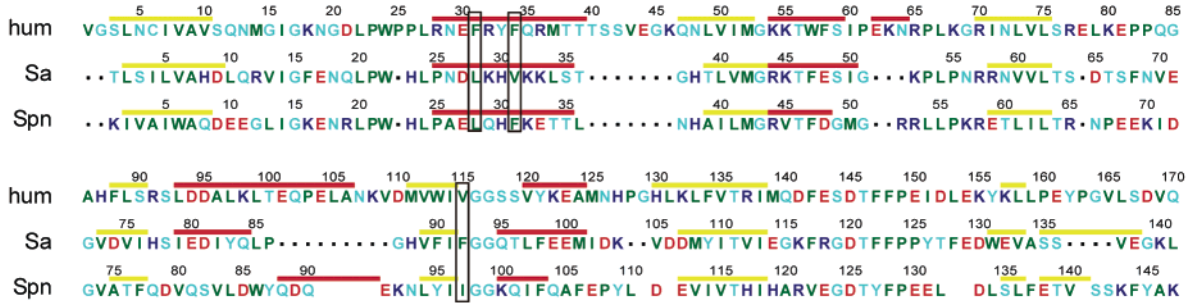

Figure 3. Sequence alignment of DHFR enzymes from three species (hum = human; Sa = *S. aureus*; Spn = *S. pneumoniae*). Crystal structures have been determined for the human and *S. aureus* enzymes, whereas the *S. pneumoniae* structure was modeled. The 16 C-terminal residues of each sequence have been omitted. Red lines denote helical regions, and yellow lines indicate β-strands as secondary structures. The three sets of highlighted residues are those mentioned in the text whose side chains are situated directly next to the 2,4-diaminopyrimidine fragment.

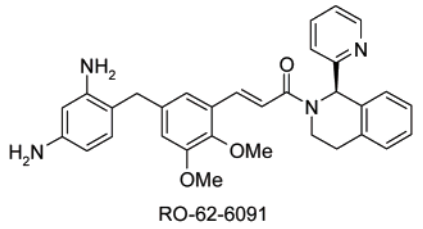

RO-62-6091

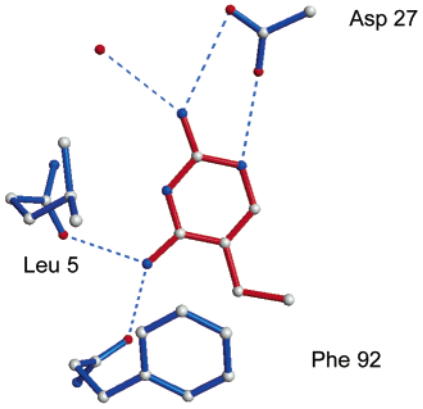

Figure 4. Structure of the Roche inhibitor whose complex structure with *S. aureus* DHFR was used for docking calculations (top) and binding mode of the 2,4-diaminopyrimidine fragment of the inhibitor that was held fixed for library docking (bottom). Details of the binding mode of the entire compound are shown in Figure 8.

performed within 2 h of CPU time on six processors of a R10k SGI Origin. FlexX produced docking solutions for about half of the library. For each of the docked compounds, the solution with the lowest score value (highest calculated binding energy) was selected. Compounds were then sorted according to their scores, and 252 out of the 300 top-ranking candidates were synthesized (library no. 1; see Table 2). In addition, 150 candidates were randomly selected from those compounds for which no docking solution could be found. This list was combined with those 150 compounds that had received the lowest docking ranks. A majority of these molecules (269 representatives) could be synthesized (library no. 2).

(b) Diversity-Based Compound Selection. In an alternative selection process, the virtual library of 9448 2,4-diaminopyrimidines was clustered according to chemical similarity. The similarity measure applied was an in-house method based on single conformers. Each pair of library molecules was superimposed at the newly formed C−N bond (bond a−b in compound **1**, Figure 2), and the amine substituent was rotated around this bond to generate conformers with maximum volume and H-bond-donor and H-bond-acceptor overlap. The list of pairwise similarity scores was used to cluster the compounds in a binary tree (complete linkage algorithm). It was found that approximately 500 compounds were needed to adequately represent the chemical space spanned by the library. A set of 501 compounds were synthesized (library no. 3).

Selection and Validation of Screening Hits. Primary selection of hits was based on activity against isolated DHFR from *S. aureus* or *S. pneumoniae* at 10 μM (>50% inhibition). Only candidates showing in addition antibacterial activity at 25 μM were selected. Further selection criteria were thymidine antagonism and activity in the presence of 10% human serum. This allowed elimination of highly hydrophobic compounds (e.g., membrane-active compounds) and those having modes of action other than DHFR inhibition. Application of these selection criteria to compounds obtained by high-throughput chemistry, and summarized in library nos. 1−3, led to the identification of a number of hits, as shown in Table 2. Most of the hit compounds identified and mentioned in Table 2 were resynthesized by classical methods, purified, characterized, and submitted to antibacterial testing. Results validated in most cases the preliminary biological data obtained by high-throughput synthesis and screening of all libraries of compounds mentioned above. They also confirmed the higher activity of this new class of inhibitors for DHFR from *S. pneumoniae* vs *S. aureus*, initially observed for the first interesting compound identified in this series (**4**). Important quantitative and qualitative differences were also observed between the different libraries. Thus, structure-based library no. 1 led to a significantly higher hit rate (21% hit rate) than diversity-based library no. 3 (3% hit rate). Library no. 2, containing compounds that had received low ranks in the docking calculation or could not be docked at all, led to only few weakly active compounds. It is important to note that the hits from library no. 1 were not biased toward activity against *S. aureus* DHFR but rather showed higher activity against *S. pneumoniae* DHFR, although a crystal structure of *S. aureus* DHFR was used for docking. This confirms our experience that the power of structure-based virtual screening generally lies in its

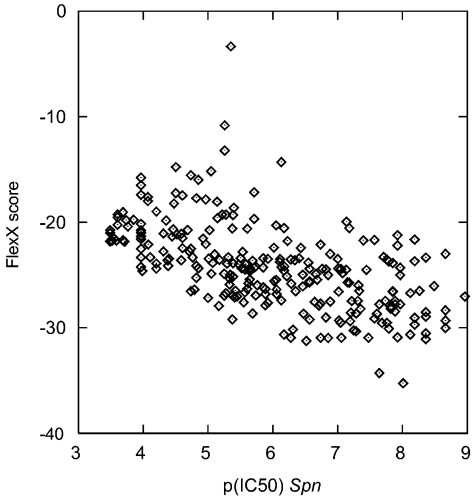

Figure 5. Correlation between FlexX score (arbitrary units) and the IC_{50} values of individual library hits against *S. pneumoniae* DHFR.

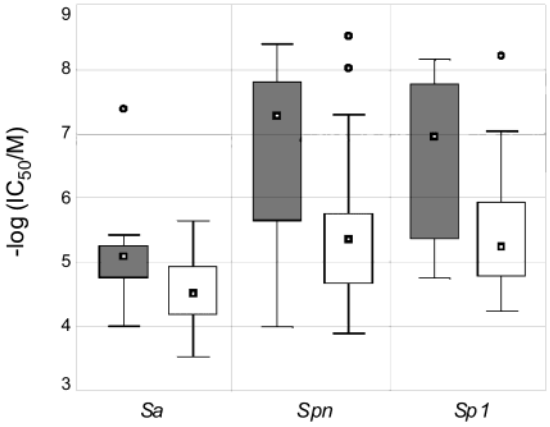

Figure 6. Box plots illustrating the activity distribution of hits from library no. 1 (shaded boxes) and library no. 3. The median is depicted as a small square. The area in the box contains all data between the 25% and 75% quantiles. Outliers beyond 1.5 times this interval are shown as open circles.

ability to filter out undesirable compounds, i.e., in excluding many inactive compounds rather than in identifying specific active ones. Specifically, FlexX does not find docking solutions for compounds with more than one bulky substituent attached to the aminomethyl nitrogen because of the steric constraints of the active site. FlexX also discards particularly small compounds and compounds with long flexible moieties. The latter are penalized by the scoring function to account for the entropic cost of conformational restriction upon binding. In contrast, FlexX assigns high ranks to 2,4-diaminopyrimidines with flat, rigid, policyclic nitrogen substituents, many of which are highly potent compounds. For example, a methylated derivative of compound **13** is rank 6 and compound **14** is rank 30 in the docking calculation (see discussion in the next section and Figure 7 below). A moderate correlation between the experimentally determined IC_{50} values against *S. pneumoniae* DHFR and the FlexX score values could be observed (Figure 5), indicating that a more stringent selection of compounds based on docking scores may have been possible, e.g., with a score cutoff of about −20. The cutoff for library no. 1, corresponding to the selection of the top 300 compounds, was approximately −13 (note that only relative score values are meaningful; the absolute values strongly depend on the details of the calculation setup and the protein structure used). Nonetheless, library no. 1 contained not only more hits but also significantly more potent hits than library no. 3. The activity ranges of resynthesized hits from library nos. 1 and 3 are displayed in Figure 6. Median values of activity between library no. 1 (shaded box) and library no. 3 differ by 2 orders of magnitude for the DHFRs from sensitive and resistant *S. pneumoniae* and by almost 1 order of magnitude for *S. aureus*. Activity against DHFR from TMP-resistant *S. aureus* was weak for all libraries. This result further underlines the efficiency of the structure-based virtual screening process.

The best inhibitors identified in library no. 1 (Table 2) are derived from amines belonging to three different chemical classes, namely, bi-, tri-, and tetracyclic amines. Therefore, an additional library (no. 4, with 370 compounds) was constructed from cyclic amines belonging to these three classes and available in our corporate collection. As expected, compounds included in library no. 4 showed high activity vs DHFR enzymes.

Structure−Activity Relationships and Structural Basis for DHFR Inhibition. A number of compounds belonging mostly to the bi-, tri-, and tetracyclic amine series showed a potent inhibitory activity mainly against TMP-sensitive and TMP-resistant DHFR from S. *pneumoniae* but less activity against *S. aureus*. Some interesting features of representatives of these classes are discussed below (Table 3 and Figure 7).

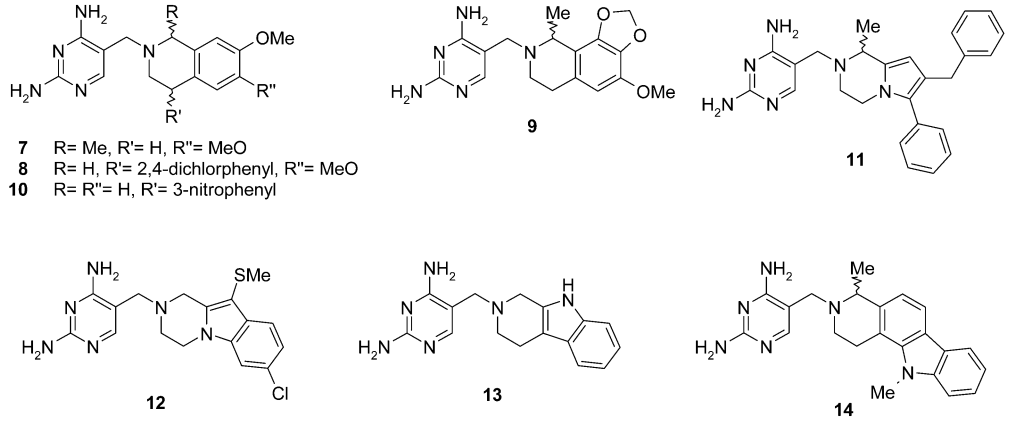

Figure 7. Individual hits from library no. 1. Activity data are summarized in Table 3.

Table 3. IC_{50} Values, Selectivity over Human DHFR, and Antibacterial Activity of Selected Compounds

compd	IC_{50} (μM)				selectivity (-fold)	MIC (μg/mL)	
	Sa	Spn	Sp1	human	human/Spn	Spn	Sp 1/1
TMP	0.027	0.075	3	900	12000	2	>64
3	40	1.1	5.5	>100	>90	8	32
4	30	0.01	0.21	30	3000	0.5	4
7	18	0.044	0.053	0.67	15	0.5	0.5
8	2	0.007	0.031	1.7	243	0.5	4
rac-**9**	9.8	0.012	0.024	1.4	117	0.25	0.5
(*S*)-**9**	5.4	0.021	0.029	0.52	25	1	2
(*R*)-**9**	1.3	0.0098	0.0028	1.2	122	0.125	0.125
10	3.2	0.006	0.056	100	16667	2	8
11	0.042	0.45	0.55	18	40	32	32
12	0.073	0.002	0.031	5.2	2600	2	4
13	7.8	0.004	0.047	180	45000	1	4
14	6.8	0.004	0.01	0.085	21	8	8

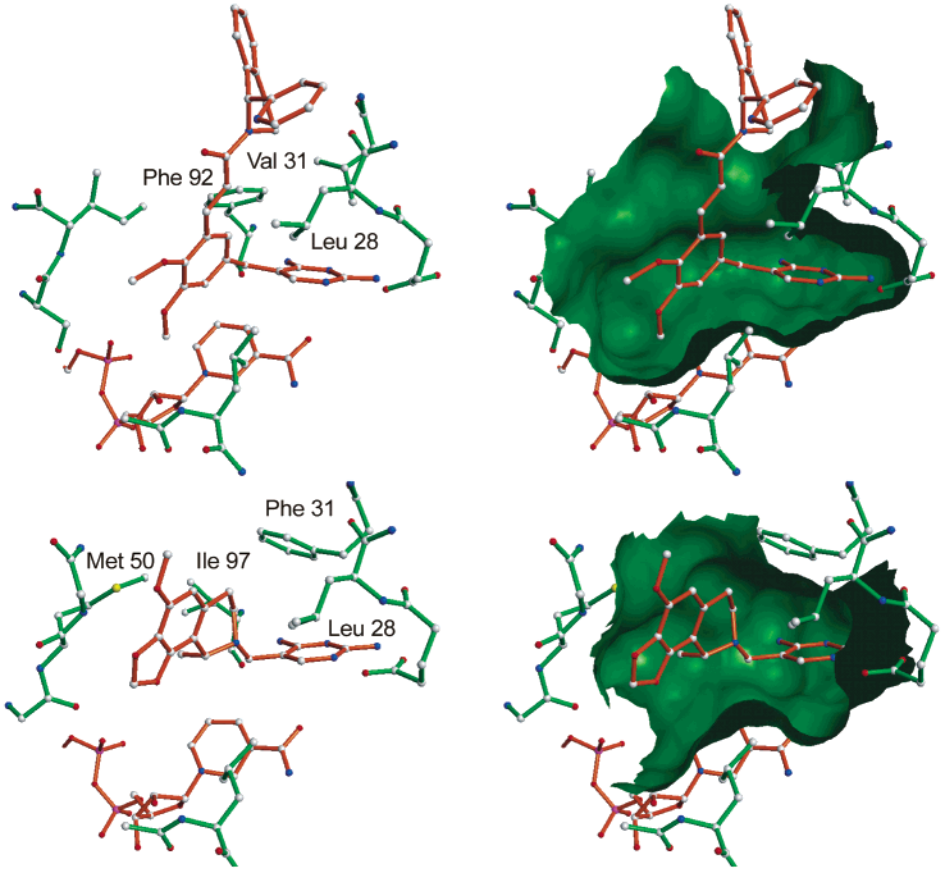

Figure 8. Binding mode of RO-62-6091 as determined by crystal structure analysis (top structures) complexed with *S. aureus* DHFR and the modeled binding mode of (*R*)-**9** (bottom structures) complexed with *S. pneumoniae* DHFR. The cofactor NADPH is partially visible at the bottom of the binding sites.

(a) Bicyclic Amines. Most compounds in this series are derived from 1,2,3,4-tetrahydroisoquinolines. It appears that the substitution pattern of the tetrahydroisoquinoline moiety plays an essential role for both potency and selectivity of the inhibitors. For instance, the unsubstituted derivative **3** is a very weak inhibitor of the DHFR from wild-type (Spn) and TMP-resistant *S. pneumoniae* (Sp1). Introduction of methoxy substituents at C-6′ and C-7′ (**4**) showed 100- and 25-fold enhancement of DHFR inhibitory activity from Spn and Sp1, respectively. Further introduction of a methyl substituent at C-1′ in compound **4** leads to a small 2- to 4-fold increase of activity (**7**). However, the presence of larger alkyl (e.g., cyclopropyl, isopropyl, and isobutyl) and aryl substituents at this position gives nearly inactive compounds. In contrast, aryl substituents at C-4′ (e.g., 2,4-dichlorophenyl) are tolerated (**8**). Tetrasubstituted derivative *rac*-**9** was identified as one of the most interesting compounds in this series. Resolution into enantiomerically pure compounds was achieved by HPLC on a chiral phase. One enantiomer showed a 10-fold higher activity against *S. pneumoniae* DHFRs. A detailed analysis of potential binding modes of both (*R*)-**9** and (*S*)-**9** was carried out by molecular modeling. It became clear that only the (*R*) isomer could fit into the DHFR active site in a manner not requiring either a strained conformation of the molecule or a slight movement of amino acid side chains in the active site. In addition, the predicted binding mode of (*R*)-**9** in the active site (Figure 8) points the methyl group in position 1 into a lipophilic pocket that is not filled by other known DHFR inhibitors. This pocket exists in all three

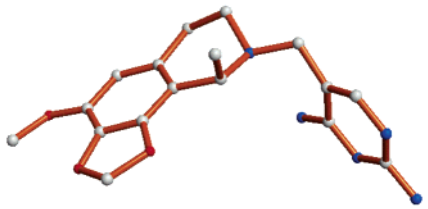

Figure 9. Crystal structure conformation of *(S)*-**9**.

DHFR isoforms. The identity of the more active enantiomer with (*R*)-**9** was confirmed by X-ray structure analysis of enantiomerically pure **9** (Figure 9).

The experimentally determined conformation of the fused ring system is virtually identical to the predicted model of the complex in Figure 8. X-ray structure analysis of racemic **9** complexed with *S. aureus* DHFR also supports this binding mode, although a high-resolution complex structure could not be obtained. A comparison of this binding mode with that of RO-62-6091 (Figure 8) shows that compound (*R*)-**9** tightly occupies the main lipophilic binding cleft extending along the plain of the 2,4-diaminopyrimidine ring system, whereas RO-62-6091 gains much of its binding energy through additional lipophilic interactions in the cleft oriented perpendicularly to the main cavity. The side chain of Met 50 in *S. pneumoniae* DHFR is oriented such that it interacts closely with the phenyl ring of the tetrahydroisoquinoline system. This interaction might be a reason for the selective inhibition of *S. pneumoniae* DHFR through the tetrahydroisoquinoline derivatives, since the human and *S. aureus* enzymes have a less polarizable isoleucin residue in this position. Still, most representatives of the tetrahydroisoquinoline series showed lower selectivity than TMP for bacteria over human DHFR, with the exception of **10**, which had comparable selectivity (16700-fold) to that of TMP (12000-fold). Finally, a single compound (**11**) showed appreciable inhibitory activity against DHFR from *S. aureus* (IC_{50} = 0.042 μM).

(b) Tricyclic Amines. A number of compounds in this series were found to be very potent inhibitors of both wild-type and TMP-resistant DHFR from *S. pneumoniae*. In addition, one of these representatives (**12**) also strongly inhibited the enzyme from TMP-sensitive *S. aureus*. Finally, compound **13** showed higher selectivity for the enzyme from *S. pneumoniae* against human source (human/Spn = 45000) than TMP itself (12000-fold).

(c) Tetracyclic Amines. Most compounds of this type (e.g., **14**) are strong inhibitors of DHFR from *S. pneumoniae* sources, but their selectivity against human DHFR is usually low.

Conclusion

A series of novel and potent inhibitors of DHFR from wild-type and TMP-resistant *Streptococcus pneumoniae* have been identified using high-throughput synthesis and screening methodology. The procedure developed for the synthesis of the novel 2,4-diaminopyrimidines is simple, efficient, and rapid. In addition, screening for enzymatic and in vitro antibacterial activity could be performed on crude reaction mixtures, thus avoiding any tedious and time-consuming purification. The library design method based on structural criteria (docking into DHFR from *Streptococcus aureus*) gave a higher hit rate and led to the identification of more potent inhibitors than diversity-based compound selection, thus allowing us to focus on the more promising candidates in a time- and cost-efficient manner.

Experimental Section

General Methods. Melting points were determined on a Buchi 510 apparatus and are uncorrected. Column chromatography was accomplished on Kieselgel 60 (70−230 mesh) obtained from E. Merck, Darmstadt. Kieselgel 60 F254 plates, also from E. Merck, were used for thin-layer chromatography, and compounds were visualized with UV light and iodine. ^{1}H nuclear magnetic resonance (NMR) spectroscopic data were recorded on a Bruker DRX 400 instrument; δ values in parts per million relative to tetramethylsilane are given. Elemental analyses are indicated by the symbol of the elements; analytical results were within 0.4% of the theoretical values.

1-[(2,4-Diamino-5-pyrimidinyl)methyl]pyridinium Bromide Monohydrobromide (6). A solution of 20.6 g (56.4 mmol) of 5-(bromomethyl)-2,4-pyrimidinediamine dihydrobromide in 170 mL of DMF was treated with 18.2 mL (225 mmol) of pyridine, and the mixture was stirred at 20 °C for 2 h, whereupon crystallization occurred. The reaction mixture was treated with 200 mL of dichloromethane, and the solids were filtered, washed with dichloromethane, and dried to give 19.7 g (96%) of **6** as a colorless solid, mp 224−226 °C. ^{1}H NMR (DMSO-d_6): δ 12.35−12.15 (1H, broad s), 9.07 (2H, d), 8.64 (1H, t), 8.8−8.3 (2H, broad s), 8.2−8.1 (3H, m), 8.1−7.7 (2H, broad s), 5.69 (2H, s). MS *m/z*: 202.2 $(M + H)^+$. Anal. ($C_{10}H_{12}N_5Br\cdot HBr$) C, H, N.

5-[(3,4-Dihydro-6,7-dimethoxy-2(1*H*)-isoquinolinyl)-methyl]-2,4-pyrimidinediamine (4). A mixture of 5-(bromomethyl)-2,4-pyrimidinediamine dihydrobromide (**5**) (365 mg, 1 mmol) and 1,2,3,4-tetrahydro-6,7-dimethoxyisoquinoline hydrochloride (690 mg, 3 mmol) in DMF (5 mL) was vigorously stirred with triethylamine (1.38 mL, 10 mmol) for 18 h. The reaction mixture was diluted with water (20 mL), and the solids were filtered, washed with water, and dried to provide **4** (245 mg, 78%) as colorless crystals, mp 235−240 °C (dec). ^{1}H NMR (DMSO-d_6): δ 7.57 (1H, s), 6.66 (1H, s), 6.63 (1H, s), 6.30 (2H, s), 5.83 (2H, s), 3.69 (3H, s), 3.67 (3H, s), 3.38 (2H, s), 3.35 (2H, signal collapsed by H_2O peak), 2.72 (2H, m), 2.61 (2H, m). MS *m/z*: 316.2 $(M + H)^+$. Anal. ($C_{16}H_{21}N_5O_2$) C, H, N.

General Procedure for the Preparation of Compounds of Type 1. Reactions were performed on a 0.7 mM scale (occasionally 0.3−0.5 mM) by treating pyridinium salt **6** with 1 equiv of primary or secondary amine in 5 mL of DMF in the presence of 5 equiv of triethylamine. After the mixture was stirred at 20 °C for 20 h, a solution was usually obtained. Evaporation of the reaction mixture to dryness, followed by column chromatography on silica gel using a mixture of dichloromethane, methanol, ammonium hydroxide and/or preparative HPLC gave pure compounds (>95%, HPLC). For some amines, **1** precipitated during the reaction and was obtained in pure form after filtration.

5-[(3,4-Dihydro-6,7-dimethoxy-1-methyl-2(1*H*)-isoquinolinyl)methyl]-2,4-pyrimidinediamine (7). Reaction of pyridinium salt **6** with 1,2,3,4-tetrahydro-6,7-dimethoxy-1-methylisoquinoline by the general procedure gave **7** as colorless crystals, mp 203−206 °C. ^{1}H NMR (DMSO-d_6): δ 7.55 (1H, s), 6.66 (1H, s), 6.63 (1H, s), 6.36 (2H, s), 5.81 (2H, s), 3.71 (1H, m, collapsed by methoxy peak), 3.70 (3H, s), 3.69 (3H, s), 3.52 (1H, d), 3.45 (1H, d), 2.95−2.45 (4H, m, partly collapsed by DMSO peak), 1.23 (3H, d). MS *m/z*: 330.4 $(M + H)^+$.

5-[[4-(2,4-Dichlorophenyl)-3,4-dihydro-6,7-dimethoxy-2(1*H*)-isoquinolinyl]methyl]-2,4-pyrimidinediamine (8). Reaction of pyridinium salt **6** with 4-(2,4-dichlorophenyl)-1,2,3,4-tetrahydro-6,7-dimethoxyisoquinoline by the general procedure gave **8** as colorless crystals, mp 118−124 °C. ^{1}H NMR (DMSO-d_6): δ 7.60 (1H, d), 7.51 (1H, s), 7.27 (1H, dd), 6.84 (1H, d), 6.78 (1H, s), 6.36 (1H, s), 5.98 (2H, s), 5.82 (2H,

s), 4.50 (1H, t), 3.71 (3H, s), 3.72−3.65 (2H, q), 3.56 (3H, s), 3.35−3.20 (2H, m), 2.77 (2H, m). MS *m*/*z*: 460.4 $(M + H)^+$.

5-[(6,9-Dihydro-4-methoxy-9-methyl-1,3-dioxolo[4,5-*h*]-isoquinolin-8(7*H*)-yl)methyl]-2,4-pyrimidinediamine (9). Reaction of pyridinium salt **6** with 6,7,8,9-tetrahydro-4-methoxy-9-methyl-1,3-dioxolo[4,5-*h*]isoquinoline by the general procedure gave (*R*,*S*)-**9** as colorless crystals, mp 191−192 °C. ^{1}H NMR (DMSO-d_6): δ 7.55 (1H, s), 6.39 (1H, s), 6.33 (2H, s), 5.98 (1H, s), 5.89 (1H, s), 5.80 (2H, s), 3.81−3.72 (1H, m, collapsed by methoxy peak), 3.77 (3H, s), 3.46−3.35 (2H, AB), 2.87−2.45 (4H, m, partly collapsed by DMSO peak), 1.19 (3H, d). MS *m*/*z*: 344.3 $(M + H)^+$. Anal. ($C_{17}H_{21}N_5O_3$) C, H, N. A 530 mg sample of (*R*,*S*)-**9** was separated by chiral HPLC (Chiracel-OD CSP 20 μm, 50 mm i.d. × 250 mm, heptane−2-propanol (1%), flow rate 60 mL/min) to yield 165 mg (*S*)-**9** and 135 mg (*R*)-**9** as colorless solids.

5-[[(9*S*)-6,9-Dihydro-4-methoxy-9-methyl-1,3-dioxolo-[4,5-*h*]isoquinolin-8(7*H*)-yl]methyl]-2,4-pyrimidinediamine: mp 205−210 °C. ^{1}H NMR (DMSO-d_6): δ 7.55 (1H, s), 6.39 (1H, s), 6.31 (2H, s), 5.98 (1H, s), 5.89 (1H, s), 5.80 (2H, s), 3.81−3.72 (1H, m, collapsed by methoxy peak), 3.77 (3H, s), 3.46−3.31 (2H, AB), 2.87−2.45 (4H, m, partly collapsed by DMSO peak), 1.19 (3H, d). MS *m*/*z*: 344.4 $(M + H)^+$. $[\alpha]_D$ +2.8° (*c* 1, $CHCl_3$).

5-[[(9*R*)-6,9-Dihydro-4-methoxy-9-methyl-1,3-dioxolo-[4,5-*h*]isoquinolin-8(7*H*)-yl]methyl]-2,4-pyrimidinediamine: ^{1}H NMR (DMSO-d_6): δ 7.55 (1H, s), 6.39 (1H, s), 6.31 (2H, s), 5.98 (1H, s), 5.89 (1H, s), 5.80 (2H, s), 3.81−3.75 (1H, m, collapsed by methoxy peak), 3.77 (3H, s), 3.46−3.31 (2H, AB), 2.87−2.45 (4H, m, partly collapsed by DMSO peak), 1.19 (3H, d). MS *m*/*z*: 344.3 $(M + H)^+$. $[\alpha]_D$ −1.9° (c 1, $CHCl_3$).

5-[[3,4-Dihydro-7-methoxy-4-(3-nitrophenyl)-2(1*H*)-isoquinolinyl]methyl]-2,4-pyrimidinediamine (10). Reaction of pyridinium salt **6** with 1,2,3,4-tetrahydro-7-methoxy-4-(3-nitrophenyl)isoquinoline by the general procedure gave **10** as yellowish crystals, mp 115 °C. ^{1}H NMR (DMSO-d_6): δ 8.06 (1H, d), 7.98 (1H, s), 7.61 (1H, d), 7.56 (1H, d), 7.53 (1H, s), 6.76 (2H, m), 6.70 (1H, dd), 5.98 (2H, s), 5.79 (2H, s), 4.37 (1H, t), 3.75−3.71 (1H, d, partly collapsed by methoxy peak), 3.71 (3H, s), 3.46 (1H, d), 3.33−3.27 (2H, AB), 2.90−2.86 (1H, dd), 2.76−2.72 (1H, dd). MS *m*/*z*: 407.4 $(M + H)^+$.

5-[[3,4-Dihydro-1-methyl-6-phenyl-7-(phenylmethyl)-pyrrolo[1,2-*a*]pyrazin-2(1*H*)-yl]methyl]-2,4-pyrimidinediamine (11). Reaction of pyridinium salt **6** with 1,2,3,4-tetrahydro-1-methyl-6-phenyl-7-(phenylmethyl)pyrrolo[1,2-*a*]pyrazine by the general procedure gave **11** as a brownish solid, mp 98−103 °C. ^{1}H NMR (DMSO-d_6): δ 7.56 (1H, s), 7.43 (2H, m), 7.31 (3H, m), 7.24 (2H, m), 7.12 (3H, m), 6.25 (2H, s), 5.82 (2H, s), 5.75 (1H, s), 3.81 (1H, d), 3.75−3.60 (5H, m), 3.07 (1H, d), 2.95−2.87,1H, m), 2.55−2.45 (1H, m, collapsed by DMSO peak), 1.40 (3H, d). MS *m*/*z*: 425.5 $(M + H)^+$.

5-[[7-Chloro-3,4-dihydro-10-(methylthio)pyrazino[1,2-*a*]indol-2(1*H*)-yl]methyl]-2,4-pyrimidinediamine (12). Reaction of pyridinium salt **6** with 7-chloro-1,2,3,4-tetrahydro-10-(methylthio)pyrazino[1,2-*a*]indole by the general procedure gave **12** as a colorless solid, mp 210−218 °C. ^{1}H NMR (DMSO-d_6): δ 7.62 (1H, s), 7.55 (2H, m), 7.14 (1H, d), 6.25 (2H, s), 5.86 (2H, s), 4.07 (2H, t), 3.79 (2H, s), 3.47 (2H, s), 2.91 (2H, t), 2.18 (3H, s). MS *m*/*z*: 375.4 $(M + H)^+$.

5-[(1,3,4,9-Tetrahydro-2*H*-pyrido[3,4-*b*]indol-2-yl)methyl]-2,4-pyrimidinediamine (13). Reaction of pyridinium salt **6** with 2,3,4,9-tetrahydro-1*H*-pyrido[3,4-*b*]indole by the general procedure gave **13** as a colorless solid, mp 205−210 °C. ^{1}H NMR (DMSO-d_6): δ 10.7 (1H, s), 7.59 (1H, s), 7.35 (1H, d), 7.25 (1H, d), 7.05−6.90 (2H, m), 6.35 (2H, s), 5.84 (2H, s), 3.53 (2H, s), 3.47 (2H, s), 2.76 (2H, s), 2.69 (2H, s). MS *m*/*z*: 295.4 $(M + H)^+$.

5-[(1,2,4,11-Tetrahydro-4,11-dimethyl-3*H*-pyrido[4,3-*a*]-carbazol-3-yl)methyl]-2,4-pyrimidinediamine (14). Reaction of pyridinium salt **6** with 2,3,4,11-tetrahydro-4,11-dimethyl-1*H*-pyrido[4,3-*a*]carbazole by the general procedure gave **14** as a colorless solid, mp 202−208 °C. ^{1}H NMR (DMSO-d_6): δ 8.05 (1H, d), 7.90 (1H, d), 7.60 (1H, s), 7.55 (1H, d), 7.40 (1H, t), 7.15 (1H, t), 6.93 (1H, d), 6.38 (2H, s), 5.82 (2H, s), 4.11 (3H, s), 3.97 (1H, q), 3.58 (1H, d), 3.52−3.40 (2H, m), 3.34 (1H, m), 3.05 (1H, m), 2.80 (1H, m), 1.37 (3H, d). MS *m*/*z*: 373.4 $(M + H)^+$.

Crystal Data for 5-[[(9*R*)-6,9-Dihydro-4-methoxy-9-methyl-1,3-dioxolo[4,5-*h*]isoquinolin-8(7*H*)-yl]methyl]-2,4-pyrimidinediamine. The compound was crystallized from an ethanol/water mixture. Crystals with dimensions 0.5 × 0.5 × 0.4 mm^3 were in orthorhombic space group *P*2(1)2(1)2(1) with a = 7.2468(14) Å, b = 14.658(3) Å, and c = 16.629(3) Å at 293 K. The 7073 reflections were measured on a SIEMENS P3 diffractometer with graphite-monochromated Cu Kα radiation. The 2385 (R_{int} = 0.0692) unique reflections were used in all calculations, and the structure was resolved by direct methods and was expanded using Fourier techniques and the program SHELX-97.[24] Non-hydrogen atoms were refined anisotropically using full-matrix least-squares refinement without restraints. The R factor and R_w factor for all data were refined to 0.0396 and 0.1032, respectively. The structure has been deposited at the Cambridge Crystallographic Data Centre, deposition number CCDC 196327.

Acknowledgment. The authors thank Andrea Araujo Del Rosario, Heidi Schlunegger, Marie-Claude Vigliano, Rémy Halm, Fabian Rufi, and David Wechsler for excellent technical assistance, Michael Hennig and Christian Oefner for X-ray structure analyses, and Paul Hadváry for his encouragement and support.

References

(1) Houvinen, P.; Sundström, L.; Swedberg, G.; Sköld, O. Trimethoprim and sulfonamide resistance. *Antimicrob. Agents Chemother.* **1995**, *39*, 279−289.

(2) Then, R. L.; Kohl, I.; Burdeska, A. Frequency and transferability of trimethoprim and sulfonamide resistance in methicillin-resistant Staphylococcus aureus and Staphylococcus epidermidis. *J. Chemother.* **1992**, *4*, 67−71.

(3) Durand, R.; Savel, J. Dihydrofolate reductase inhibitors: New developments in antiparasitic chemotherapy. *Expert Opin. Ther. Pat.* **2001**, *11*, 1285−1290.

(4) Wyss, P. C.; Guerry, P.; Hartman, P. G.; Hubschwerlen, C.; Jolidon, S.; Locher, H.; Specklin, J.-L.; Stalder, H. Anti-MRSA Dihydrofolate Reductase Inhibitors: Synthesis and SAR. Presented at the 39th Interscience Conference on Antimicrobial Agents and Chemotherapy, San Francisco, CA, September 26−29, 1999; Abstract No. 1800.

(5) Matthews, D. A.; Bolin, J. T.; Burridge, J. M.; Filman, D. J.; Volz, K. W.; Kaufman, B. T.; Beddell, C. R.; Champness, J. N.; Stammers, D. K.; Kraut, J. Refined crystal structures of *Escherichia coli* and chicken liver dihydrofolate reductase containing bound trimethoprim. *J. Biol. Chem.* **1985**, *260*, 381−391.

(6) Dauber-Osguthorpe, P.; Roberts, V. A.; Osguthorpe, D. J.; Wolff, J.; Genest, M.; Hagler, A. T. Structure and energetics of ligand binding to proteins: *Escherichia coli* dihydrofolate reductase−trimethoprim, a drug−receptor system. *Proteins* **1988**, *4*, 31−47.

(7) Boehm, H.-J.; Boehringer, M.; Bur, D.; Gmuender, H.; Huber, W.; Klaus, W.; Kostrewa, D.; Kuehne, H.; Luebbers, T.; Meunier-Keller, N.; Mueller, F. Novel inhibitors of DNA gyrase: 3D structure based biased needle screening, hit validation by biophysical methods, and 3D guided optimization. A promising alternative to random screening. *J. Med. Chem.* **2000**, *43*, 2664−2674.

(8) Godel, T.; Riemer, C.; Edenhofer, A. Preparation of pyrimidines for treatment and/or prevention of illnesses caused by disorders of the dopamine system. Patent WO 9713759, 1997.

(9) Daluge, S. M.; Skonezny, P. M.; Roth, B.; Rauckman, B. S. Antibacterial pyrimidine compounds. Patent EP 96214, 1983.

(10) Huber, W. 2,4-Diamino-5-(4-methyl-5-β-hydroxyethylthiazolium chloride)methylpyrimidine hydrochloride, a new analog of thiamin. *J. Am. Chem. Soc.* **1943**, *65*, 2222−2226.

(11) Tieckelmann, H.; Guthrie, R.; Nain, J. G. 2,4-Diamino-5-formylpyrimidine and 2,4-diamino-5-hydroxymethylpyrimidine. *J. Org. Chem.* **1960**, *25*, 1257−1259.

(12) Weinstock, L. T.; O'Brien, D. E.; Cheng, C. C. Folic acid analogs. I. p{[(2,4-Diamino-5-pyrimidinyl)methyl]amino}benzoyl-L-glutamic acid and related compounds. *J. Med. Chem.* **1968**, *11*, 1238−1241.

(13) Stuart, A.; Paterson, T.; Roth, B.; Aig, E. 2,4-Diamino-5-benzylpyrimidines and analogues as antibacterial agents. 6. A one-step synthesis of new trimethoprim derivatives and activity analysis by molecular modeling. *J. Med. Chem.* **1983**, *26*, 667−673.
(14) *Methods for Dilution Antimicrobial Susceptibility Tests for Bacteria That Grow Aerobically*, 3rd ed.; National Committee for Clinical Laboratory Standards: Villanova, Pa, 1993; Vol. 13, No. 25, Article M7-A3.
(15) Dale, G. E.; Broger, C.; D'Arcy, A.; Hartmann, P. G.; DeHoogt, R.; Jolidon, S.; Kompis, I.; Labhardt, A. M.; Langen, H.; Locher, H.; Page, M. G. P.; Stüber, D.; Then, R. L.; Wipf, B.; Oefner, C. A single amino acid substitution in *staphylococcus aureus* dihydrofolate reductase determines trimethoprim resistance. *J. Mol. Biol.* **1997**, *266*, 23−30.
(16) Sadowski, J.; Rudolph, C.; Gasteiger, J. Automatic generation of 3D atomic coordinates for organic molecules. *Tetrahedron Comput. Methodol.* **1990**, *3*, 537−547.
(17) Sadowski, J.; Schwab, C. H.; Gasteiger, J. *Corina*; Molecular Networks GmbH Computerchemie: Erlangen, Germany, 1998.
(18) Clark, M.; Cramer, R. D., III; Van Opdenbosch, N. Validation of the general purpose Tripos 5.2 force field. *J. Comput. Chem.* **1989**, *10*, 982−1012.
(19) Rarey, M.; Kramer, B.; Lengauer, T.; Klebe, G. A fast flexible docking method using an incremental construction algorithm. *J. Mol. Biol.* **1996**, *261*, 470−489.
(20) Rarey, M.; Wefing, S.; Lengauer, T. Placement of medium-sized molecular fragments into active sites of proteins. *J. Comput.-Aided Mol. Des.* **1996**, *10*, 41−54.
(21) Rarey, M.; Kramer, B.; Lengauer, T. Multiple automatic base selection: Protein−ligand docking based on incremental construction without manual intervention. *J. Comput.-Aided Mol. Des.* **1997**, *11*, 369−384.
(22) Rarey, M.; Kramer, B.; Lengauer, T. Docking of hydrophobic ligands with interaction-based matching algorithms. *Bioinformatics* **1999**, *15*, 243−250.
(23) Stahl, M. Modifications of the scoring function in FlexX for virtual screening applications. *Perspect. Drug Discovery Des.* **2000**, *20*, 83−98.
(24) Sheldrick, G. M. Phase annealing in SHELX-90: direct methods for larger structures. *Acta Crystallogr.* **1990**, *A46*, 467−473.

JM020495Y